Cathodoluminescence microscopy of superconducting and non-superconducting Tl2Ba2CuO6+x polycrystals

C. Diaz-Guerra, J. Piqueras, Christine Opagiste

C. Diaz-Guerra, J. Piquera and C. Opagiste, Physica C 259 (1996) 121-130

Cathodoluminescence microscopy of superconducting and non-superconducting $Tl_2Ba_2CuO_{6+x}$ polycrystals

C. Diaz-Guerra[a], J. Piqueras[a] and C. Opagiste[b]

[a] *Departamento de Fisica de Materiales, Facultad de Ciencias Fisicas, Universidad Complutense, E-28040 Madrid, Spain*
[b] *Laboratoire Structure de la Matière, Université de Savoie, B.P.240, 9 Rue de L'Arc-en-Ciel, F-74942 Annecy le Vieux, Cedex, France*

Abstract

Luminescence properties of $Tl_2Ba_2CuO_{6+x}$ samples with different superconducting transition temperatures have been studied by cathodoluminescence (CL) in the scanning electron microscope. Independent of the crystal structure, tetragonal or orthorhombic, the CL spectra show two resolved bands at about 430 nm (2.9 eV) and 540 nm (2.3 eV), respectively. The results show that the 2.3 eV emission is related to oxygen content and is more intense in low-oxygen content superconducting samples. It is proposed that this band is related to a complex center involving oxygen vacancies. A comparison of spectra from $Tl_2Ba_2CuO_{6+x}$ and from precursors used in the synthesis (CuO_x, $Tl_2Ba_20_5$) has been carried out.

1. Introduction

The luminescence of different high-temperature superconductors (HTSC's) has been studied by a number of authors in the past years. Investigations of ceramic or crystalline samples of $YBa_2Cu_30_{7-x}$ (YBCO), $Bi_2Sr_2CaCu_20_x$ (BSCCO) and $Tl_2Ba_2CuO_{6+x}$ (TBCO) have revealed similar luminescence spectral features suggesting that the emission bands are related to structural properties, as the existence of Cu-O planes, common to the mentioned materials. Visible luminescence has been mainly observed in the blue-green spectral range [1-12] often showing well resolved bands peaked at about 430 nm (2.9 eV) and 540 nm (2.3 eV). The luminescence emission of samples without post-preparation treatment is in general weak and the 430 nm bands dominate the spectra. This band is considered to be intrinsic to the abovementioned HTSC systems and has been attributed in the case of YBCO and BSCCO to an oxygen quasi-molecule [8] or to a complex involving F center and negative molecular oxygen ion in YBCO [10]. The band has been also observed in TBCO samples prepared under high pressure at high temperature [11]. The 540 nm band has a rather complex behavior. It is absent in untreated YBCO and BSCCO but appears after different thermal or irradiation treatments. In particular, an increase of cathodoluminescence (CL) emission under high-excitation conditions in the scanning electron microscope has been reported in YBCO and BSCCO studies[1-3,7,12,13]. Spectral analysis shows that this effect is mainly due to the appearance or drastic increase of the 540 nm band although the emission at 430 nm also increases [7,12]. The increase of the 540 nm emission has been also observed after laser irradiation or vacuum annealing. Since the mentioned treatments cause a variation in the oxygen stoichiometry or distribution, the possibility that the 540 nm luminescence is related to mechanisms in the oxygen sub-lattice has been investigated. Miller et al. [14] reported an increase of CL signal in oxygen-depleted zones of YBCO produced by electron irradiation. Similar effects were reported in Refs. [3] and [7]. In Ref. [7] a correlation between irradiated oxygen-depleted zones - as detected by micro

Raman spectroscopy - and enhanced 540 nm CL emission, was observed. A further study of YBCO sintered samples prepared with different oxygen contents [12] revealed that oxygen depletion alone does not cause the appearance of strong 540 nm emission. In fact the band appears during controlled electron irradiation in the scanning microscope in oxygen-poor samples but not in samples with full or high oxygen content. This observation leads to the conclusion that the centers causing the 540 nm emission in YBCO involve oxygen vacancies but are formed only after irradiation or annealing treatments similar for instance to the F centers in ionic crystals.

The 540 nm band has been also reported in TBCO [11] but contrary to that observed in YBCO and BSCCO this luminescence is already present in as prepared sintered samples. A complete characterization of the TBCO samples used in Ref. [11] has shown that 540 nm luminescence is inhomogeneous in the sample and is not related to impurity phases but to regions with variations in the oxygen content. The fact that no post-preparation treatment is necessary to detect the 540 nm band in TBCO makes this material very suitable to study the origin of this band and in particular the influence of the oxygen stoichiometry on this and other luminescence bands. To this purpose the luminescence properties of $Tl_2Ba_2CuO_{6+x}$ samples with different superconducting transition temperatures have been investigated in this work. Since the crystallographic structure of $Tl_2Ba_2CuO_6$ is either orthorhombic (Ccc2) [15] or tetragonal I4/mmm [16] and both phases are superconducting with Tc between 0 and 92 K [18,19], we have studied samples of both structures.

2. Experimental method

The synthesis procedure of the samples has been described in detail in Refs. [17] and [20]. $Tl_2Ba_20_5$ and CuO_x powders were used as starting components. Two different batches were prepared from a stoichiometric amount of powders. For batch A the powder were first kept for three days at 750°C under 1 bar oxygen whereas batch B was not pre-treated. The powder mixture was pressed under 5 kbar into pellets, then placed in a furnace under 100 bar of argon or of oxygen and the appropriate thermal treatment was given. In the first case tetragonal superconducting (TS) samples are obtained while the treatment under oxygen yields orthorhombic non-superconducting (ONS) samples. A series of annealing treatments at low oxygen pressure have shown that starting samples with different symmetry i.e. ONS and TS transform into orthorhombic superconducting, indicating that the final state of the specimens does not depend on the initial symmetry. In this work the three samples whose codes and relevant data are listed in Table 1 have been studied. One sample (TM-850) is tetragonal superconducting, one (TKO-930) is orthorhombic non-superconducting and the last (TH2-850b) is orthorhombic and superconducting.

Samples from batch A are X-ray pure. Some traces of CuO and $Ba_2Cu_30_x$ impurities are detected; both are estimated to be < 0.1% by volume. Optical micrographs show only T1-2201 grains. The samples from batch B contain, besides the 2201 stoichiometric grains, less than 5% by volume of starting $Tl_2Ba_20_5$ impurity phase and very small CuO grains (< 0.1% by volume). Further details on these samples are described in Refs. [17] and [20].

Samples were polished with diamond paste but, for comparison, also non-polished surfaces were investigated. The samples were observed in the emissive and CL modes in a Hitachi S-2500 scanning electron microscope at accelerating voltages of 20-30 kV and temperatures between 80 and 300 K. For CL measurements an optical lens was used to concentrate the light on a photomultiplier attached to a window of the microscope. To record spectra a light guide feeding the light to an Oriel 78215 computer controlled monochromator was used. It has been observed in different luminescent materials that CL spectra recorded with focused and defocused electron beam are different as a consequence of the presence of radiative centers with a low concentration. For this reason CL spectra were recorded under different focusing conditions of the electron beam on the samples.

Table 1
Relevant physical parameters of the samples investigated

Sample	Batch	T_c (K)	f (%)	Symmetry	a (Å)	b (Å)	c (Å)
TM-850	B	91.1	43.9	14/mmm	3.8717	3.8717	23.225
TH2-850b	B	52.4	49.1	Ccc2	5.4582	5.4811	23.213
TKO-930	A	0	–	Ccc2	5.4467	5.4911	23.144

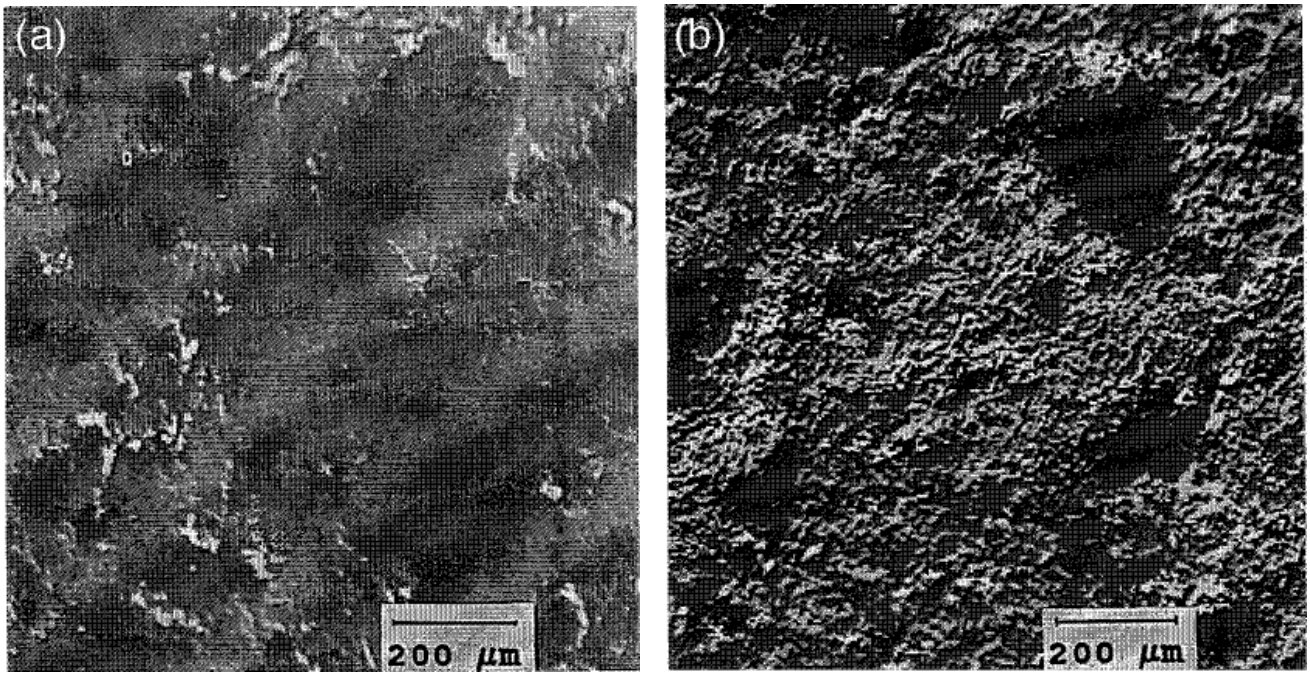

Fig. 1: (a) Panchromatic CL image of an unpolished surface of the superconducting TH2-850b sample and (b) the corresponding secondary image.

3. Results

3.1. Microscopy of $Tl_2Ba_2CuO_6$

The general appearance of emissive mode and CL images is similar in the three samples studied. Fig. 1 shows a typical emissive image of an unpolished surface and the panchromatic CL image. An inhomogeneous distribution of luminescence, not related to specific topographic features is observed. The polished surfaces, Fig. 2, show many pores in the topographic image which correspond to regions of enhanced CL intensity. In order to check if this effect is due to particles related to the mechanical polishing treatment which remain in the pores after cleaning the sample, the inner surfaces of a number of pores were observed at higher magnification. Inside the pores well defined grain surfaces and no foreign particles are observed. These microscopy results indicate that the enhanced CL in the pores is related to grain surfaces, freshly exposed during the polishing treatment.

3.2. CL spectroscopy of $Tl_2Ba_2CuO_6$

Luminescence spectra have been found to depend on the sample considered, on the state of the surface (polished or unpolished), on temperature and on the excitation conditions (focused or unfocused electron beam). In the following, representative results are described with some emphasis on the behavior of the 430 nm (2.9 eV) and 540 nm (2.3 eV) luminescence bands and on the comparison between the different samples.

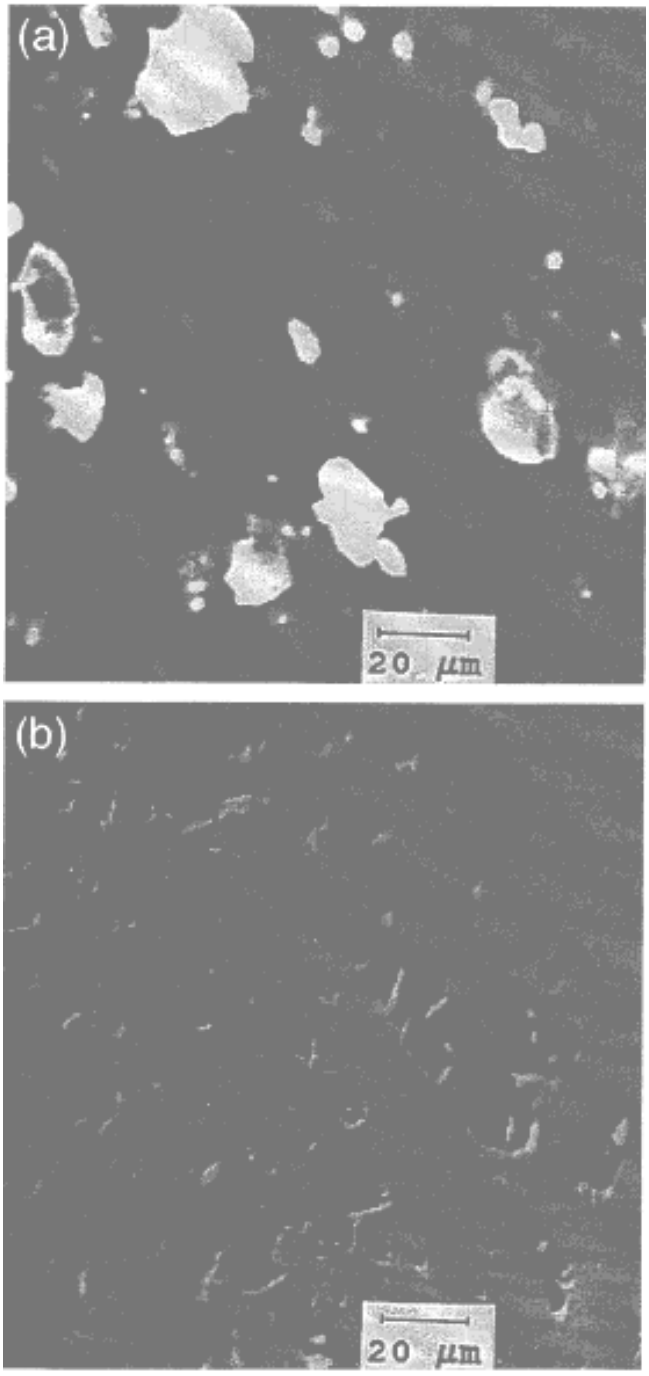

Fig. 2 : (a) Panchromatic CL image of the polished surface of the TH2-850b superconducting sample and (b) the corresponding secondary image.

3.2.1. Spectra of unpolished surfaces

Cross-sections of the sintered samples have been used as unpolished surfaces. In the same samples the upper polished surfaces were studied as described in the next section.

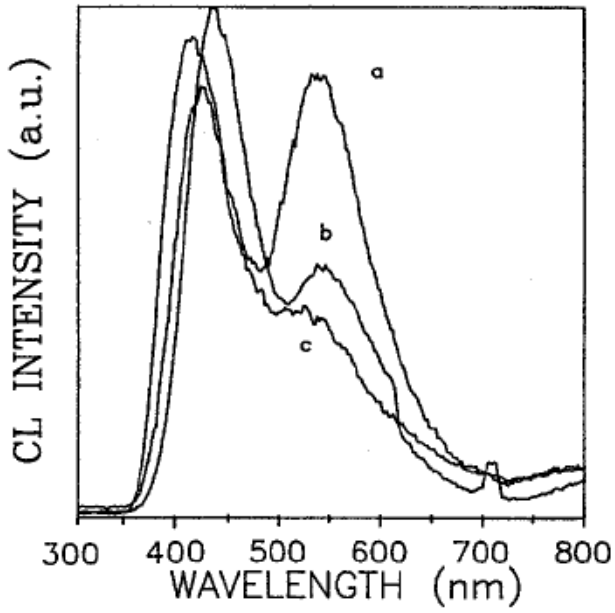

Fig. 3 :. CL spectra recorded under focused electron beam at the unpolished surfaces of the three samples at 80 K. (a) TM-850 superconducting sample, (b) TH2-850b superconducting sample, (c) TKO 930 non-superconducting sample.

Fig. 3 shows the spectra recorded in unpolished surfaces of the three samples at 80 K. Two bands centered, respectively, at about 430 nm and 540 nm are observed. In the non-superconducting sample the 540 nm emission is not well resolved as a separate band while the 430 nm one dominates. In the TH2- 850b sample (T c = 52.4 K) both bands are well resolved and the intensity of the 430 nm band is still higher. In the TM-850 sample (T~ = 91.1 K) both bands are of comparable intensity. These results indicates a relative increase of the 540 nm band by increasing the critical temperature Tc of the sample.

Fig. 4 shows the temperature dependence of the spectra of sample TM-850. The total intensity increases with decreasing temperature and the relative weight of the bands changes. A temperature decrease favors the appearance of a well resolved 430 nm band. From room temperature to approximately 200 K the 540 nm emission is stronger than the 430 nm blue one. A similar behavior of the CL spectra with

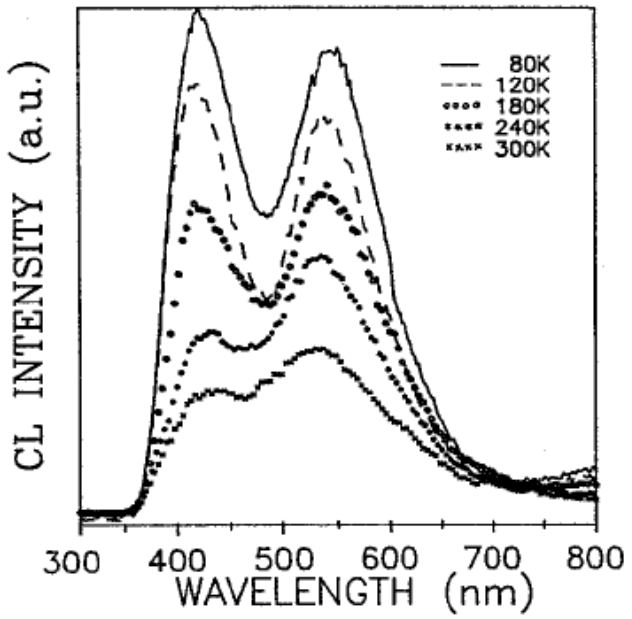

Fig. 4. Temperature dependence of the CL spectra of TM-850 superconducting sample.

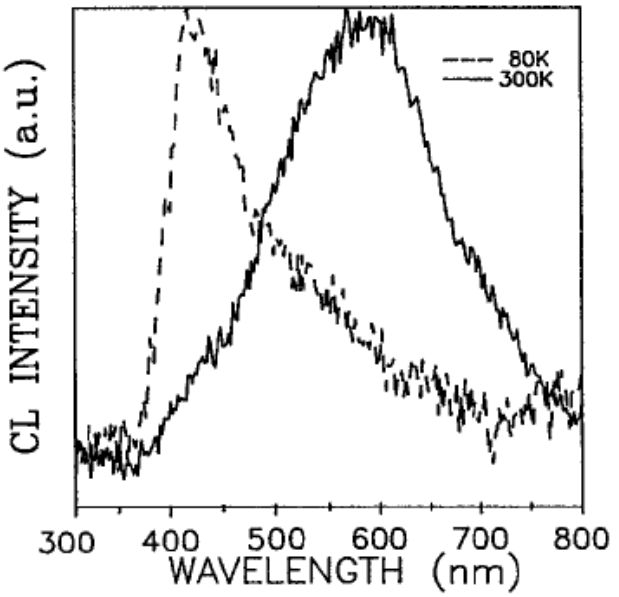

Fig. 5. CL spectra from a bright area of the TH2-850b superconducting sample at different temperatures.

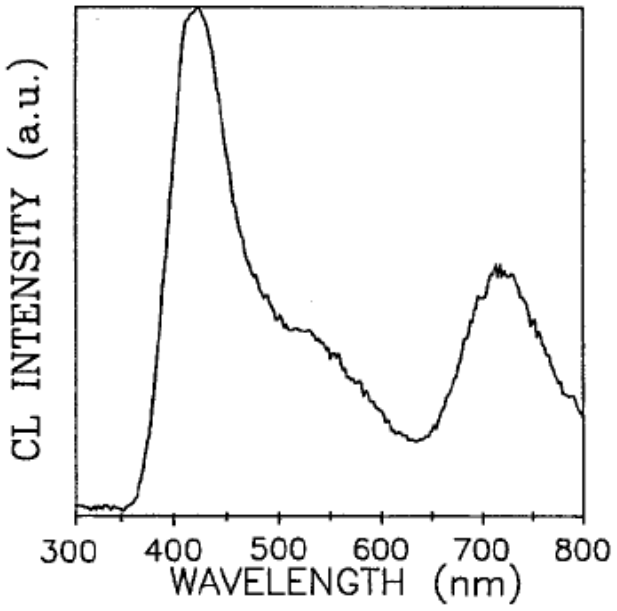

Fig. 6. Low-tempera~re (80 K) eL spectrum from a highly luminescent area of the non-superconducting TKO 930 sample.

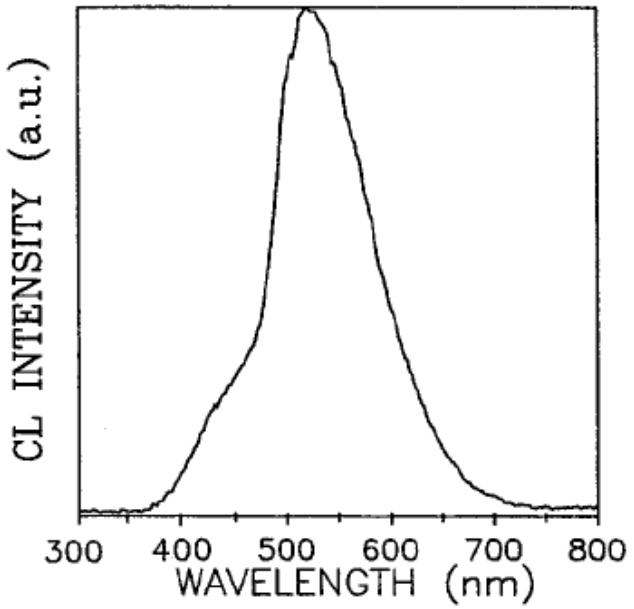

Fig. 7. CL emission spectrum recorded in a pore of TH2-850b superconducting sample.

temperature was also found in the other samples investigated. Spectra of Figs. 3 and 4 were recorded under excitation with a focused electron beam and correspond to an area of the sample including bright and dark regions of the corresponding CL image.

Some differences in the spectra are observed when a defocused electron beam is used or when specific areas of the sample are chosen. In particular, defocusing the electron beam (i.e. reducing the excitation density) causes a relative increase of the green (540 nm) band. On the other side, spectra recorded in highly luminescent areas of the superconducting sample TH2-850b (Fig. 5) show at low temperature only the 420 nm band extending in the green region, and at room temperature a broad band centered between 580 and 600 nm. The low-temperature spectra of the highly luminescent areas of the non-superconducting sample show in addition a well

resolved band peaked at 720 nm (Fig. 6).

3.2.2. Spectra of polished surfaces

The highly luminescent regions in polished surfaces correspond to pores, as observed in the CL images (Fig. 2). Spectral analysis shows that emission from the pores is mainly due to the 540 nm band. Fig. 7 shows the spectrum recorded during excitation with focused electron beam in a pore of sample TH2-850b. In this figure the 540 nm band is dominant and the higher-energy emission appears as a shoulder. As in the case of unpolished surfaces, defocusing causes an increase of the green band in the pores of the superconducting samples.

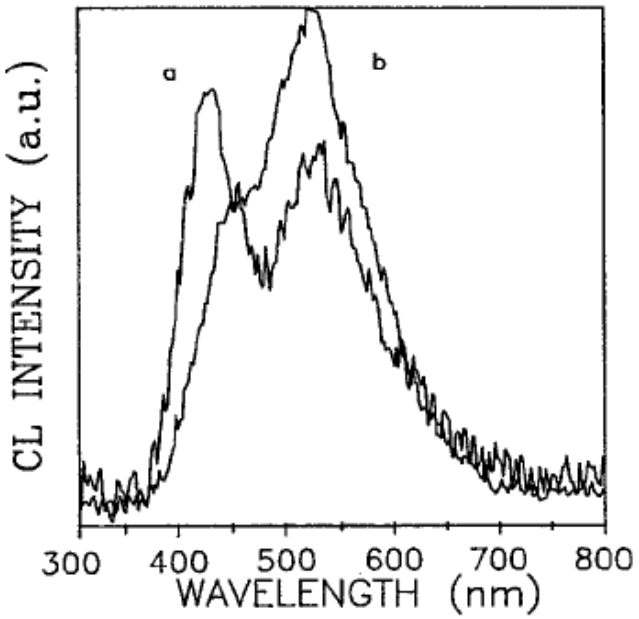

Fig. 8. CL spectra from the polished surface of TKO 930 non-superconducting sample, recorded at 80 K in (a) a non-porous area, (b) a porous area.

Spectra recorded in large areas, including pores and polished material, generally show a dominant 540 nm green band as well as emission in the blue region which appears as a shoulder of the main band and whose relative intensity increases by decreasing temperature. As in the spectra of the unpolished surfaces the relative contribution of this green emission increases with the Tc value of the sample. In the non-superconducting sample the shape of the spectra shows a strong dependence on the porosity of the considered area. In porous regions the contribution of the 430 nm band is often higher than in both superconducting samples. Fig. 8 shows spectra of different areas in the TKO-930 sample. It is observed that the relative intensity of the 430 nm blue band is high as compared with the spectrum of the superconducting sample shown in Fig. 7.

3.3. CL spectroscopy of precursors

In the polished surface of the CuO_x sample the spectrum shown in Fig. 9 with two bands centered at about 445 and 530 nm, respectively, is recorded. Unpolished surfaces show a more complicated spectrum (Fig. 10) with a broad band extending from 400 to 670 nm and a well resolved band peaked at about

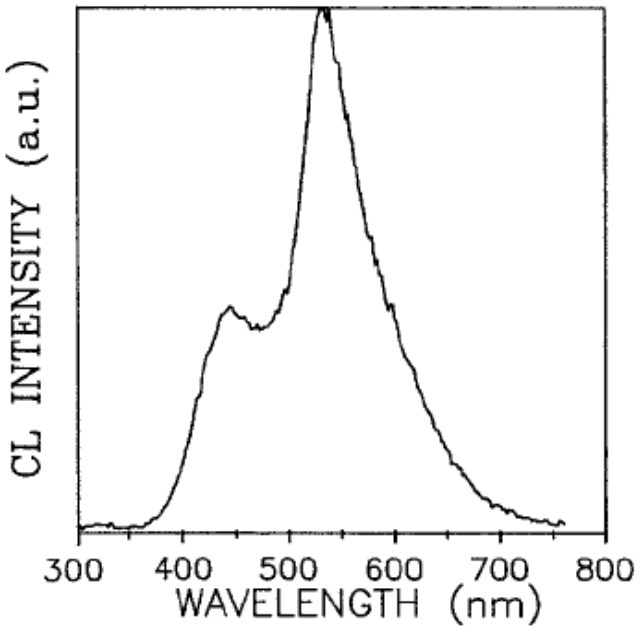

Fig. 9. CL spectrum from the polished surface of a CuO_x precursor sample.

730 nm. The lower the temperature the stronger is the red emission.

Under some excitation conditions a component of the broad band at about 590-600 nm appears well resolved. The broad band contains probably the three components at 440 nm, 530 nm and 590-600 nm.

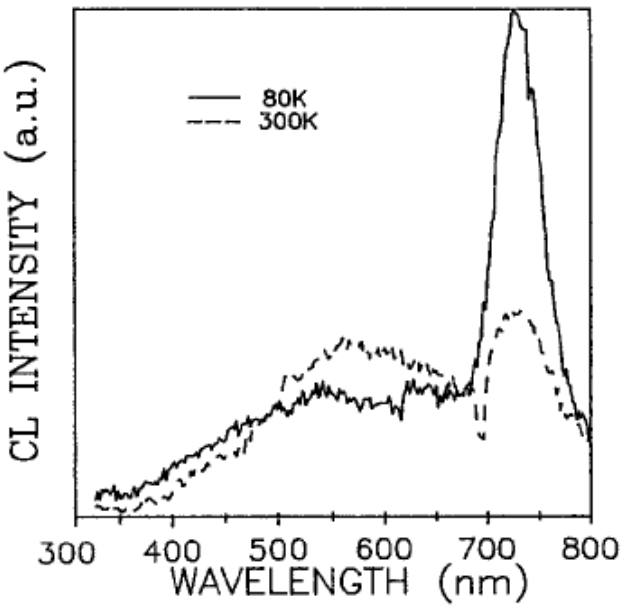

Fig. 10. CL emission spectra from an unpolished surface of a CuO_x sample at several temperatures.

Fig, 11 shows spectra at different temperatures of the $Tl_2Ba_20_5$ precursor. Two well resolved bands at about 420 and 550 nm, respectively, are observed. The total emission is higher at low temperatures, specially the 550 nm band.

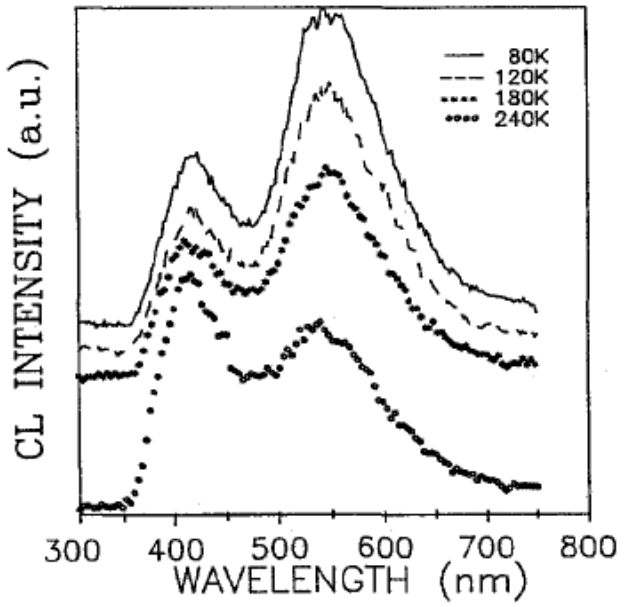

Fig. 11. Temperature dependence of the CL spectra of the $Tl_2Ba_20_5$ precursor. (Spectra have been shifted for convenience.)

4. Discussion

CL images of all samples reveal the existence of luminescence emission with an inhomogeneous spatial distribution. This observation, which agrees with the previous results referred to in Section 1, is independent of the superconducting properties of the samples and on their crystal structure - tetragonal or orthorhombic. The general appearance of CL images, shown in Figs. 1 and 2 for polished and unpolished surfaces, respectively, is similar for samples corresponding to batches A and B although the impurity phase content has been found to differ markedly in both batches. According to the available information on the impurity phases in the samples [17,20,21] the inhomogeneous distribution of the CL intensity cannot be attributed to these impurities. The two phases present in batch A samples appear in a very small amount as compared with the extension of bright regions in the CL image. Previous characterization [21] by different techniques has shown that these samples contain regions extending hundreds of microns which contain only 2201 grains without significant variations of the cation stoichiometry. In the batch B sample the volume of the impurity phase is higher [20,21] due to the presence of unreacted $Tl_2Ba_20_5$ precursor inclusions, but the amount is lower than 5% in volume. The similarity of CL images of the three samples (two of batch B and one of batch A) and the fact that emission is distributed all over the sample enables one to rule out that the localized $Tl_2Ba_20_5$ inclusions have a significant influence on the CL observed in the batch B samples. This point will be later discussed in view of the spectral response of the precursors. In the following we discuss the possible origin of the emission as an intrinsic effect of the $Tl_2Ba_2CuO_6$, not related to impurity phases.

To our knowledge, intrinsic luminescence of $Tl_2Ba_2CuO_6$ has been only reported in our previous work [11] on a superconducting sample similar to the TM-850 used in this one. CL inhomogeneity has been attributed to local variations of the oxygen content, influencing the intensity of the 530 nm band. As described above,

a similar relationship between 530 nm emission and oxygen content has been reported for YBCO samples. On the other hand, models proposed for the 430 nm emission, e.g. Refs. [8] and [10], also involve processes with oxygen atoms or oxygen vacancies. For these reasons, the possibility that features in the oxygen sublattice determine or influence the spectral response of the different samples used in this work is considered here. In particular, the samples differ in oxygen content as a result of mass losses during synthesis process. From EDAX and plasma emission spectroscopy measurements it has been concluded [17,20,21] that the high-Tc tetragonal sample (TM-850) has a lower oxygen content than the orthorhombic non-superconducting sample (TKO-930). The difference between the samples has been estimated to an amount of 0.4 per formula unit. The other sample investigated (TH2-850b) has an intermediate Tc value (52.4 K) and is partially oxy genated [20]. As Fig. 3 shows a decrease in oxygen content is related to a relative intensity increase of the 540 nm band. Such a correlation has been observed in YBCO samples [7,12] and leads to the conclusion that centers causing a 540 nm emission involve oxygen vacancies. The present observations support this possibility as proposed also in Ref. [11]. A difference between the YBCO samples described in Refs. [7] and [11] and the $Tl_2Ba_2CuO_6$ used here is that in the former the 540 nm emission appears only after irradiation or annealing treatments while in the latter the band is observed without post-synthesis treatments. It is proposed that the 530-540 nm emission is related to a complex center involving oxygen vacancies. The center - as the F type center in ionic crystals - would be formed after specific treatments in YBCO while in the $Tl_2Ba_2CuO_6$ appears during the particular high-temperature synthesis process used. Comparison of results on YBCO and $Tl_2Ba_2CuO_6$ shows that the intensity of the 530-540 nm band is not related to the superconducting behavior (Tc) of the sample but to the oxygen content. In YBCO, the band is more intense in low-oxygen non-superconducting samples [7,12] and in $Tl_2Ba_2CuO_6$ the intensity is higher in low-oxygen superconducting samples. The relationship between the 540 nm band and oxygen content also explains the inhomogeneity of the luminescence revealed by CL images, which would be due to an inhomogeneous oxygen concentration in the sample [11]. This effect is used to explain [21] the reduced superconducting volume fraction (f= 45%) of the superconducting samples of this work.

The 540 nm band shows an increase, relative to the 420 nm band when a defocused electron beam (low excitation density) is used. A similar effect has been observed in other HTSC samples as well as in semiconducting materials. In the latter, deep-level emission bands are in many cases enhanced by defocusing the microscope electron beam, see, e.g., Refs. [22] and [23] as a consequence of the presence of radiative centers with a low concentration. In the spectra recorded under conditions of defocused beam the correlation between oxygen content and intensity of the 540 nm band is maintained. Comparison between spectra from polished and unpolished surfaces of the same sample shows a higher relative intensity of the green band after polishing. The above described effect of an enhanced 540 nm band intensity by decreasing oxygen content applies when samples with the same surface state - polished or unpolished - are compared.

The 420 nm band, which is also related to processes in the oxygen sublattice, has a different origin than the 540 nm emission, as revealed by the different temperature dependence of both bands (Fig. 4), the different response to changes in excitation density and by the decrease of the 420 nm band by surface polishing (Fig. 7). The presence of the 420 nm band in all samples studied in this work agrees with similar observations in YBCO and BSCCO and supports the proposal [8,10] of its intrinsic character. In our experiments we could not determine if the relative enhancement of the 540 nm in polished surfaces is due to generation of the corresponding centers or to a quenching effect influencing mainly the 420 nm emission. In any case the surface state has to be considered when comparison among different samples is performed.

In addition to the sample dependence of the relative intensity of the 540 nm band, other

minor, mostly space-localized differences, have been detected. For instance in some bright areas of the TH2-850b sample the 420 nm band is clearly dominant at low temperature, as the spectrum of Fig. 5 shows. The same observation applies to the polished non-superconducting sample in which the inner surfaces of the pores show strong 420 nm emission (Fig. 8). While such an effect is probably related to the strong inhomogeneity of the intrinsic luminescent centers, other spectral features would be due to impurity phases. This is the case of the well resolved band at 720 nm (Fig. 6) observed in small, well localized regions of the non-superconducting sample (TKO-930). A band at the same wavelength has been reported in Cu_2O [24,25] and was attributed to oxygen vacancies. As Fig. 10 shows this band is also observed in unpolished surfaces of the CuO_x precursors used in the preparation of our $Tl_2Ba_2CuO_6$ samples. This indicates that the regions showing 720 nm emission include CuO_x precursor.

In polished CuO_x the red emission is quenched and the spectrum of Fig. 9 with bands centered at about 440 and 540 nm is recorded. The spectrum is very similar to the spectra of $Tl_2Ba_2CuO_6$ sample and to previously reported CL spectra of YBCO and BSCCO. Since emission in $Tl_2Ba_2CuO_6$ is not due to CuO_x inclusions, as discussed above, the analogy could be related to the common structural features of HTSC's and copper oxides. In particular the basic structural unit of CuO is similar to the CuO_2 layers in HTSC's. On the other hand CuO is a charge-transfer insulator [26] and super-conducting cuprates show charge-transfer excitations between O 2p and Cu 3d states, see e.g. Refs. [27-30].

$Tl_2Ba_2O_5$ impurities have been only detected in the samples of batch B and consequently they do not determine the luminescence features common to the three samples studied in this work. However, since we are not aware of previous luminescence work on $Tl_2Ba_2O_5$ we recorded its CL spectra at different temperatures in view to future works related to this precursor and HTSC materials. As Fig. 11 shows, $Tl_2Ba_2O_5$ has emission bands at 400-420 nm and 540-560 nm. Contrary to that observed in $Tl_2Ba_2CuO_6$, the relative intensity of the 540-560 nm band increases by decreasing temperature.

5. Conclusions

The luminescence emission of the $Tl_2Ba_2CuO_{6+X}$ samples investigated shows an inhomogeneous spatial distribution not related to impurity phases. This result applies to superconducting and non-superconducting material and does not depend on the crystal structure, tetragonal or orthorhombic. A band at 540 nm (2.3 eV) is related to the oxygen content. It increases with reducing oxygen content and it is proposed to be due to a complex center involving oxygen vacancies. Another band centered at about 430 nm (2.9 eV), previously attributed to processes in the oxygen sublattice, has a different origin than the 540 nm emission. Comparison with the luminescent behavior of the precursors, CuO_x and $Tl_2Ba_2O_5$, shows common features in the spectra of $Tl_2Ba_2CuO_{6+x}$ and CuO_x.

Acknowledgements

CDG acknowledges MEC for a FPI research grant. This work has been supported by DGICYT (Project PB93-1256).

References

[1] V.N. Andreev, B.P. Zakharchenya, S.E. Nikitin, F.A. Chudnovskii, E.B. Shadim and E.M. Ster, JETP Lett. 46 (1987) 492.
[2] B.J. Luff, P.D. Townsend and J. Osborne, J. Phys. D 21 (1988) 663.
[3] J. Piqueras, P. Fernfiadez and J.L. Vicent, Appl. Phys. Lett. 57 (1990) 2722.
[4] I. Ya Fugol, V.N. Samovarov, Yu. I. Rybalko and V.M. Zhuravlev, Mod. Phys. Lett. B 4 (1990) 803.
[5] V. Ya Yaskolko, L.N. Oster and K.M. Mukinov, Phys. Status Solidi A 123 (1991) K35.
[6] A. Rem6n, J.A. Garcia, P. G6mez, J. Piqueras and F. Domlnguez-Adame, Phys. Status Solidi A 136 (1993) K127.

[7] P. G6mez, J. Jimenez, P. Martin, J. Piqueras and F. Dominguez-Adame, J. Appl. Phys. 74 (1993) 6289.
[8] V.G. Stankevitch, N. Ya. Svechnikov, K.V. Kaznacheev, M. Kamada, S. Tanaka, S. Hirose, R. Kink, G.A. Emel'chenko, S.G. Karahachev, T. Wolf, H. Berger and F. Levy, Phys. Rev. B 42 (1993) 1024.
[9] J.A. Garcia, A. Rem6n and J. Piqueras, Phys. Status Solidi A 144, (1994) 217.
[10] I. Fugol, C. Politis, A. Ratner, V. Samovarov and V. Zhuravlev, J. Lumin. 62 (1994) 291.
[11] P. G6mez, J. Piqueras and C. Opagiste, Solid State Commun. 91 (1994) 747.
[12] P. G6mez, J. Piqueras, M. Sayagues and J.M. Gonzalez-Calbet, Solid State Commun. 96 (1995) 45.
[13] F. Dominguez-Adame, P. Fernandez, J. Piqueras, P. Prieto, C. Barrero and M.E. G6mez, J. Appl. Phys. 71 (1992) 2778.
[14] J.H. Miller, J.D. Huhn, S.L. Holder, A.N. DiBianea and C.R. Bagnelly, Appi. Phys. Lett. 56 (1990) 89.
[15] A.W. Hewat, P. Bordet, J.J. Capponi, C. Chaillout, J. Cheneras, M. Godinho, E.A. Hewat, J.L. Hodeau and M. Marezio, Physica C 156 (1988) 369.
[16] Y. Shimakwa, Y. Kubo, T. Manako, H. Igurashi, F. Izumi and H. Asano, Phys. Rev. B 42 (1990) 101654.
[17] C. Opagiste, M. Couach, A.F. Khoder, R. Abraham, T.K. Hondo, J.L. Jorda, M. Th. Cohen-Adad, A. Junod, G. Triscone and J. Muller, J. Alloys Comp. 195 (1993) 47.
[18] Y. Shimakawa, Y. Kubo, T. Manako and H. Igarashi, Physica
C 185-189 (1991)639.
[19] Y. Shimakawa, Physica C 204 (1993) 247.
[20] C. Opagiste, G. Triscone, M. Couach, T.K. Jondo, J.L. Jorda, A. Junod, A.F. Khoder and J. Muller, Physica C 213 (1993) 17.
[21] C. Opagiste, M. Couach, A.F. Khoder, T. Graf, A. Junod, G. Triscone, J. Muller, T.K. Jondo, J.L. Jorda, R. Abraham, M.Th. Cohen - Adad, L.A. Bursill, O. Leckel and M.G. Blanchin, Physica C 205 (1993) 247.
[22] U. Pal, P. Fernandez, J. Piqueras, N.V. Sochinskii and E. Dieguez, J. Appl. Phys. 78 (1995) 1992.
[23] H.C. Casey and J.S. Jayson, J. Appl. Phys. 42 (1971) 2774.
[24] J. Bloem, A.J. Van der Houver van Oort and F.A. Kroger, Physica 22 (1956) 1254.
[25] R. Gilbert Kaufman and R.T. Hawkins, J. Electrochem. Soc. 133 (1986) 2652.
[26] J. Ghijsen, L.H. Tjeng, J. van Elp, H. Eskes, J. Westerink and G.A. Sawatzky, Phys. Rev. B 38 (1988) 11322.
[27] S. Tajima, H. Ishii, T. Nakahoshi, T. Takazi, S. Uchida, M. Seki, S. Sugu, Y. Hidaka, M. Suzuki, T. Murukami, K. Oka and H. Unoki, J. Opt. Soc. Am. B 6 (1989) 475.
[28] J.J. Yeh, I. Lindau, J.Z. Sun, K. Chas, N. Missert, A. Kapitulnik, T.H. Geballe and M.R. Beasley, Phys. Rev. B 42 (1990) 8044.
[29] S. Tajima, Appl. Supercond. 1 (1993) 313.
[30] E. Dagotto, Rev. Mod. Phys. 66 (1994) 763.